Diarylborenium Cations: Synthesis, Structure, and Electrochemistry

Ching-Wen Chiu and François P. Gabbaï*

Department of Chemistry, Texas A&M University, College Station, Texas 77843

Received December 14, 2007

Summary: Mes_2BF and $Ar^N{}_2BF$ (Ar^N = 4-(Me_2N)-2,6-Me_2-C_6H_2) react with trimethylsilyltriflate and p-dimethylaminopyridine in chlorobenzene to afford the corresponding borenium salts $[Mes_2B\text{-}DMAP]^+$ OTf^- ($[\mathbf{1}]^+OTf^-$) and $[Ar^N{}_2B\text{-}DMAP]^+$ OTf^- ($[\mathbf{2}]^+OTf^-$), which have been fully characterized.

Introduction

Cationic boron derivatives continue to attract a great deal of attention because of their instability and reactivity.[1–6] Diphenylborenium cations of general formula $[Ph_2B\text{-}L]^+$ (L = neutral ligand) provide a good example of such species, which had long been proposed but whose definitive characterization in solution has only recently been achieved.[7–11] Despite these recent successes, diphenylborenium cations have not been structurally characterized. Furthermore, the acridine-9-borafluorenium cation is the only structurally characterized example of a diarylborenium cation.[12] The difficulties encountered in the isolation of such cations can be correlated to the unsaturation of the boron center and the weak π-donating ability of the aryl groups. In an effort to overcome these limitations, we have probed the use of more sterically protecting aryl substituents featuring *o*-methyl groups. We have also probed the stabilizing effects that can be provided by remote amino-substituents appended to the aryl groups of diarylborenium cartions.[13]

Results and Discussion

The reaction of Mes_2BF with trimethylsilyl triflate (Me_3SiOTf) and *p*-dimethylaminopyridine (DMAP) in refluxing chlorobenzene affords after 24 h $[Mes_2B\text{-}DMAP]^+OTf^-$ ($[\mathbf{1}]^+OTf^-$) (Scheme 1).[14] In an effort to determine the effect of remote amino-substituents on the stability of such borenium ions, we also synthesized $Ar^N{}_2BF$ (Ar^N = 4-(Me_2N)-2,6-Me_2-C_6H_2) and converted it into $[Ar^N{}_2B\text{-}DMAP]^+OTf^-$ ($[\mathbf{2}]^+OTf^-$) by following the method used for $[\mathbf{1}]^+OTf^-$. The formation of $[\mathbf{1}]^+OTf^-$ and $[\mathbf{2}]^+OTf^-$ was confirmed by ^1H NMR, which showed the presence of one DMAP ligand bound to the boron center. The ^1H NMR spectra of $[\mathbf{1}]^+OTf^-$ and $[\mathbf{2}]^+OTf^-$ are also different from those of $[Mes_2BF\text{-}DMAP]$ and $[Ar^N{}_2BF\text{-}DMAP]$, respectively, which could be generated in situ by simple mixing of the diarylboron fluoride with DMAP. Of special note, the ^1H NMR resonance of the Me_2N group of DMAP is shifted downfield by 0.36 ppm on going from $[Mes_2BF\text{-}DMAP]$ to $[\mathbf{1}]^+OTf^-$ and 0.31 ppm on going from $[Ar^N{}_2BF\text{-}DMAP]$ to $[\mathbf{2}]^+OTf^-$. These observation are in agreement with an ionic formulation for $[\mathbf{1}]^+OTf^-$ and $[\mathbf{2}]^+OTf^-$. This was confirmed by the detection of a ^{11}B NMR signal at 64 ppm for $[\mathbf{1}]^+OTf^-$ and 62 ppm for $[\mathbf{2}]^+OTf^-$. These chemical shifts are comparable to the value reported for $[(C_6H_5)_2B(Py)]^+$ (58.2 ppm) which also feature a tricoordinate boron atom.[11] While $[\mathbf{1}]^+OTf^-$ is isolated as colorless crystals, $[\mathbf{2}]^+OTf^-$ is an orange solid.

Scheme 1

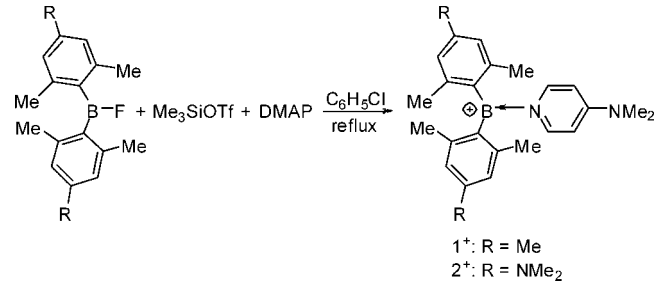

Bearing in mind that the only structurally characterized diarylborenium salt features a fused 9-borafluorenium moiety,[12] we undertook the characterization of $[\mathbf{1}]^+OTf^-$ and $[\mathbf{2}]^+OTf^-$ by X-ray analysis. Both salts crystallize in the $P\bar{1}$ space group with two molecules in the unit cell. Both structures are very similar (Figure 1). The boron center of $[\mathbf{1}]^+OTf^-$ and $[\mathbf{2}]^+OTf^-$ is trigonal planar as indicated by the sum of the bond angles, which is equal to 360° in both cases. The B(1)−C(8) (1.560(3)Å in $[\mathbf{1}]^+$, 1.550(4) Å in $[\mathbf{2}]^+$) and B(1)−C(18) bonds (1.570(3)Å in $[\mathbf{1}]^+$, 1.532(4) Å in $[\mathbf{2}]^+$) connecting the aryl ligand to the boron centers are significantly shorter than the C_{Mes}−B bonds measured in Mes_2BPh (1.579(2) Å),[15] suggesting increased π-donation to the electron-deficient boron center. The average

* Corresponding author. E-mail: francois@tamu.edu. Fax: +1 979 845 4719. Phone: + 1 979 862 2070.

(1) Kölle, P.; Nöth, H. *Chem. Rev.* **1985**, *85*, 399.
(2) Piers, W. E.; Bourke, S. C.; Conroy, K. D. *Angew. Chem., Int. Ed. Engl.* **2005**, *44*, 5016.
(3) (a) Vidovic, D.; Findlater, M.; Cowley, A. H. *J. Am. Chem. Soc.* **2007**, *129*, 8436. (b) Vidovic, D.; Findlater, M.; Cowley, A. H. *J. Am. Chem. Soc.* **2007**, *129*, 11296.
(4) Braun, U.; Nöth, H. *Eur. J. Inorg. Chem.* **2007**, 2296.
(5) Kato, T.; Tham, F. S.; Boyd, P. D. W.; Reed, C. A. *Heteroatom Chem.* **2006**, *17*, 209.
(6) Chiu, C.-W.; Gabbai, F. P. *Angew. Chem., Int. Ed. Engl.* **2007**, *46*, 1723.
(7) Davidson, J. M.; French, C. M. *J. Chem. Soc.* **1962**, 3364.
(8) Moodie, R. B.; Ellul, B.; Connor, T. M. *Chem. Ind.* **1966**, *1966*, 767.
(9) Kiyooka, S.-I.; Fujiyama, R.; Kawai, T.; Fujimoto, H.; Goh, K. *Tetrahedron Lett.* **2001**, *42*, 4151.
(10) Uddin, M. K.; Fujiyama, R.; Kiyooka, S.-i.; Fujio, M.; Tsuno, Y. *Tetrahedron Lett.* **2004**, *45*, 3913.
(11) Uddin, M. K.; Nagano, Y.; Fujiyama, R.; Kiyooka, S.-i.; Fujio, M.; Tsuno, Y. *Tetrahedron Lett.* **2005**, *46*, 627.
(12) Narula, C. K.; Nöth, H. *Inorg. Chem.* **1985**, *24*, 2532.
(13) Schulz, A.; Kaim, W. *Chem. Ber.* **1989**, *122*, 1863.
(14) These reaction conditions are those employed in the self-activated silyl-assisted poly-onio-substitution protocol developed by Robert Weiss, see for example: Weiss, R.; Puhlhofer, F. G. *J. Am. Chem. Soc.* **2007**, *129*, 547.
(15) Fiedler, J.; Zalis, S.; Klein, A.; Hornung, F.; Kaim, W. *Inorg. Chem.* **1996**, *35*, 3039.

10.1021/om701249n CCC: $40.75 © 2008 American Chemical Society
Publication on Web 03/08/2008

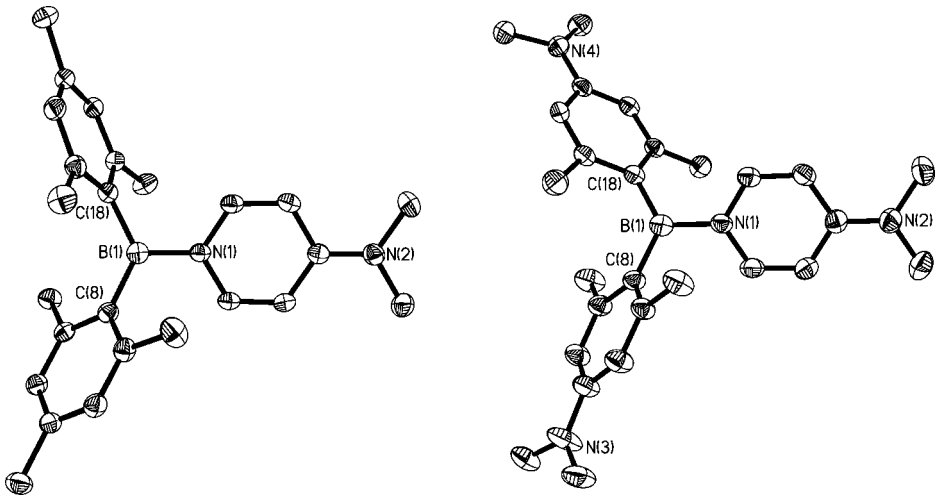

Figure 1. Crystal structure of $[\mathbf{1}]^+$ and $[\mathbf{2}]^+$ with thermal ellipsoids set at the 50% probability level. Hydrogen atoms are omitted for clarity. Pertinent metrical parameters can be found in the text.

dihedral angles θ formed between the boron trigonal plane and the plane containing the Mes ligand in $[\mathbf{1}]^+$ and the Ar^N ligand in $[\mathbf{2}]^+$ are respectively 58.1° and 48.3°. The slight shortening of the B(1)−C(8) and B(1)−C(18) bonds as well as the smaller θ angle observed for $[\mathbf{2}]^+$ may be correlated to the stronger π-donating ability of the Ar^N ligand, a conclusion supported by the planarity of the N(3) and N(4) atoms ($\Sigma_{(C\text{-}N\text{-}C)} = 359.8°$ (N(3)) and 358.2° (N(4))). The B(1)−N(1) bonds connecting the DMAP ligand to the boron centers (1.480(3)Å in $[\mathbf{1}]^+$, 1.501(4) Å in $[\mathbf{2}]^+$) in both structures are shorter that the value computed for $[(C_6H_5)_2B(Py)]^+$ (1.552 Å).[11] They are also shorter than the $B-N_{DMAP}$ bond observed in Ar*P═B(DMAP)Tmp (Ar* = C_6H_3-2,6-(C_6H_2-2,4,6-iPr_3)$_2$; Tmp = 2,2,6,6-tetramethylpiperidine) and are in fact comparable to traditional B−N single bonds.[16,17] The electron deficiency of the cationic boron center as well as the strong σ-donor character of the DMAP ligand are most certainly responsible for this feature.

In an attempt to better understand the properties of $[\mathbf{1}]^+$ and $[\mathbf{2}]^+$, we have studied their electrochemistry. As indicated by cyclic voltammetry, both $[\mathbf{1}]^+$ and $[\mathbf{2}]^+$ undergo an irreversible reduction at E_{peak} −2.03 and −2.30 V (vs Fc/Fc^+), respectively (Figure 2). Because of their increased electron deficiency, the reduction potentials of $[\mathbf{1}]^+$ and $[\mathbf{2}]^+$ are more positive than that of neutral boranes, such as Mes_3B, which is reduced at −2.73 V (vs Fc/Fc^+). It is also important to note that the reduction potential of $[\mathbf{1}]^+$ is substantially more positive than that of $[\mathbf{2}]^+$ once again indicating the greater donating ability of the Ar^N ligand. The redox behavior of these derivatives is different from that of neutral boranes which typically display a reversible one-electron reduction wave corresponding to the formation of stable radical anion.[18] Hence, these results indicate that the radical $[Mes_2B\text{-}DMAP]^\bullet$ and $[Ar^N{}_2B\text{-}DMAP]^\bullet$ are not stable. It also suggests that radicals such as $[Mes_2B\text{-}pyridine]^\bullet$ whose generation has been attempted[19] might be too unstable to actually observe in solution.[20]

A geometry optimization of $[\mathbf{1}]^+$ and $[\mathbf{2}]^+$ with DFT methods (B3LYP, 6-31G*) affords structures that closely match those

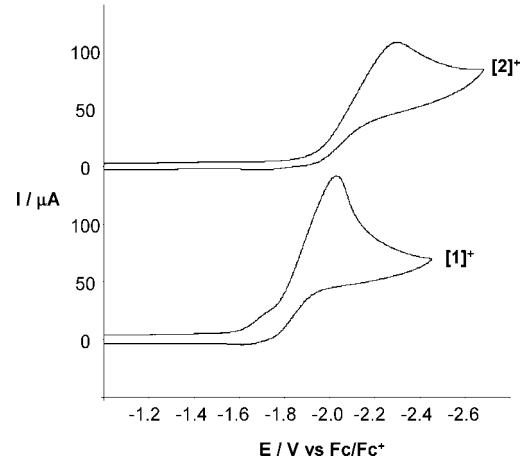

Figure 2. Cyclic voltammograms of $[\mathbf{1}]^+$ and $[\mathbf{2}]^+$ in CH_2Cl_2 with a glassy-carbon working electrode (0.1 M nBu_4NPF_6) at scan rate of 300 mV s^{-1}.

observed experimentally. In both cases, the LUMO is localized on the boron atom and DMAP ligand (Figure 3). An evaluation of the orbital energies by using the PCM solvation model[21,22] (solvent = CH_2Cl_2) indicates that the LUMO of $[\mathbf{1}]^+$ is 0.37 eV lower than that of $[\mathbf{2}]^+$. This energy difference is close to the results of our electrochemical measurements (ΔE_{peak}(red) = 0.27 V).

Experimental Section

General Considerations. Trimethylsilyl triflate (Me_3SiOTf) was purchased from TCI America and used without purification. *p*-Dimethylaminopyridine (DMAP) was purchased from Lancaster and used without purification. 4-Bromo-3,5-tetramethylaniline was synthesized by following a published procedure.[23] Chlorobenzene was dried over P_2O_5 under N_2 atmosphere and distilled prior to

(16) Rivard, E.; Merrill, W. A.; Fettinger, J. C.; Power, P. P. *Chem. Commun.* **2006**, 3800.
(17) Rivard, E.; Merrill, W. A.; Fettinger, J. C.; Wolf, R.; Spikes, G. H.; Power, P. P. *Inorg. Chem.* **2007**, *46*, 2971.
(18) Cummings, S. A.; Iimura, M.; Harlan, C. J.; Kwaan, R. J.; Trieu, I. V.; Norton, J. R.; Bridgewater, B. M.; Jäkle, F.; Sundararaman, A.; Tilset, M. *Organometallics* **2006**, *25*, 1565.
(19) Leffler, J. E.; Dolan, E.; Tanigaki, T. *J. Am. Chem. Soc.* **1965**, *87*, 927.
(20) Weissman, S. I.; van Willigen, H. *J. Am. Chem. Soc.* **1965**, *87*, 2285.
(21) Cossi, M.; Barone, V.; Cammi, R.; Tomasi, J. *Chem. Phys. Lett.* **1996**, *255*, 327.
(22) Tomasi, J.; Cammi, R.; Mennucci, B. *Int. J. Quantum Chem.* **1999**, *75*, 783.
(23) Engman, L.; Stern, D.; Stenberg, B. *J. Appl. Polym. Sci.* **1996**, *59*, 1365.

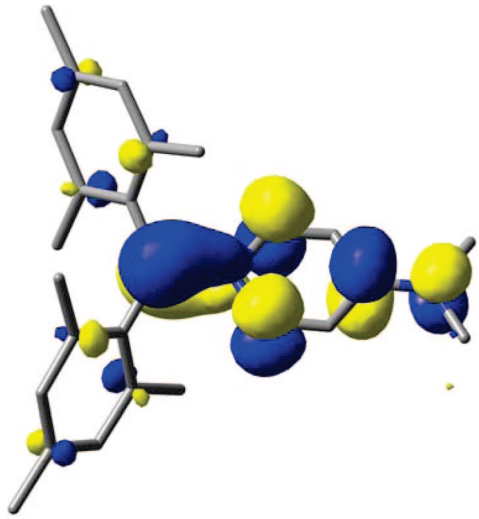

Figure 3. DFT optimized geometry of $[\mathbf{1}]^+$ with an overlay of the LUMO (isovalue = 0.03, H-atoms omitted).

use. Air-sensitive compounds were handled under N_2 atmosphere, using standard Schlenk and glovebox techniques. Elemental analyses were performed at Atlantic Microlab (Norcross, GA). NMR spectra were recorded on a Varian Unity Inova 400 FT NMR spectrometer (399.59 MHz for ^{1}H, 375.95 MHz for ^{19}F, 128.2 MHz for ^{11}B, 100.5 MHz for ^{13}C). Chemical shifts δ are given in ppm, and are referenced against external Me_4Si (H, ^{13}C), $BF_3 \cdot Et_2O$ (^{11}B), and $CFCl_3$ (^{19}F).

Synthesis of $Ar^N{}_2BF$ (Ar^N = 4-(Me_2N)-2,6-Me_2-C_6H_2). 4-Bromo-3,5-tetramethylaniline (10 g, 0.04 mol) was allowed to react with excess Mg powder in THF (30 mL) at reflux for 5 h. Once the reaction mixture was cooled to room temperature, the THF solution was filtered and then slowly added into an Et_2O solution of $BF_3 \cdot OEt_2$ (2.7 mL, 0.02 mol) at −78 °C. The reaction mixture was allowed to warm to room temperature and stirred overnight. The solvents were then removed under reduced pressure and the solid residue was extracted with hexane (3 × 50 mL). The combined hexane fractions were dried under vacuum to afford a yellow solid. This solid was washed with hexane (5 mL) to afford $Ar^N{}_2BF$ in moderate yield (3.8 g, 53%). This compound was used without further purification for the synthesis of $[\mathbf{2}]^+OTf^-$ (vide infra). ^{1}H NMR ($CDCl_3$, 399.59 MHz): δ 2.39 (d, 12H, *o*-Me), 3.06 (s, 12H, Ar^N-NMe_2), 6.46 (s, 4H, Ar^N-CH). ^{13}C NMR ($CDCl_3$, 100.5 MHz): δ 23.2 (*o*-Me), 40.0 (Ar^N-NMe_2), 111.3, 125.6, 144.4, 151.6. ^{19}F NMR ($CDCl_3$, 375.95 MHz): δ −23.4. ^{11}B NMR ($CDCl_3$, 128.2 MHz): δ 52.

Synthesis of $[\mathbf{1}]^+OTf^-$. Dimesitylboron fluoride (0.60 g, 2.2 mmol), DMAP (0.23 g, 1.9 mmol), and Me_3SiOTf (0.34 mL, 1.9 mmol) were dissolved in 5 mL of chlorobenzene and heated at reflux overnight to give a colorless solution. Upon cooling, compound $[\mathbf{1}]^+OTf^-$ precipitated and was isolated as a white solid by filtration. It was washed with Et_2O (10 mL) and dried under reduced pressure (0.78 g, 80% yield). Single crystals were obtained by slow cooling a hot chlorobenzene solution of $[\mathbf{1}]^+OTf^-$ to −40 °C. ^{1}H NMR ($CDCl_3$, 299.91 MHz): δ 2.01 (s, 12H, *o*-Me), 2.30 (s, 6H, *p*-Me), 3.43 (s, 6H, DMAP-NMe_2), 6.87 (s, 4H, Mes-CH), 7.00 (d, 2H, $^3J_{H\text{-}H}$ = 7.8 Hz, DMAP-CH), 7.87 (d, 2H, $^3J_{H\text{-}H}$ = 7.8 Hz, DMAP-CH). ^{13}C NMR ($CDCl_3$, 100.5 MHz): δ 21.3 (*o*-Me), 22.5 (*p*-Me), 41.3 (DMAP-NMe_2), 109.2, 122.3, 129.3, 133.2, 142.2, 143.9, 158.1. ^{11}B NMR ($CDCl_3$, 128.2 MHz): δ 64. Anal. Calcd for $C_{26}H_{32}BF_3N_2O_3S$: C, 60.01; H, 6.20. Found: C, 59.36; H, 6.16. The sample could be further purified by an additional recrystallization from hot chlorobenzene. Anal. Calcd for $C_{26}H_{32}BF_3N_2O_3S$: C, 60.01; H, 6.20. Found: C, 60.16 H, 6.19.

Synthesis of $[\mathbf{2}]^+OTf^-$. $Ar^N{}_2BF$ (0.28 g, 0.85 mmol), DMAP (0.08 g, 0.65 mmol), and Me_3SiOTf (0.11 mL, 0.61 mmol) were dissolved in 5 mL of chlorobenzene and heated at reflux overnight to give an orange solution. After cooling to room temperature, addition of Et_2O (20 mL) resulted in the precipitation of $[\mathbf{2}]^+OTf^-$ as an orange solid that was isolated by filtration. It was washed with Et_2O (10 mL) and dried under reduced pressure (0.24 g, 69% yield). Single crystals were obtained by vapor diffusion of Et_2O into a $CHCl_3$ solution of the $[\mathbf{2}]^+OTf^-$. ^{1}H NMR ($CDCl_3$, 399.59 MHz): δ 1.94 (s, 12H, *o*-Me), 2.98 (s, 12H, Ar^N-NMe_2), 3.36 (s, 6H, DMAP-NMe_2), 6.32 (s, 4H, Ar^N-CH), 6.91 (d, 2H, $^3J_{H\text{-}H}$ = 8.0 Hz, DMAP-CH), 7.89 (d, 2H, $^3J_{H\text{-}H}$ = 8.0 Hz, DMAP-CH). ^{13}C NMR ($CDCl_3$, 100.5 MHz): δ 23.4 (*o*-Me), 39.8 (Ar^N-NMe_2), 40.9 (DMAP-NMe_2), 108.5, 111.7, 144.3, 152.4, 157.9. ^{11}B NMR ($CDCl_3$, 128.2 MHz): δ 62. Anal. Calcd for $C_{28}H_{38}BF_3N_4O_3S$: C, 58.13; H, 6.62. Found: C, 57.60; H, 6.56.

Electrochemistry. Electrochemical experiments were performed with an electrochemical analyzer from CH Instruments (Model 610A) with a glassy carbon working electrode and a platinum auxiliary electrode. The reference electrode was built from a silver wire inserted into a small glass tube fitted with a porous vycor frit at the tip and filled with a THF solution containing $(n\text{-}Bu)_4NPF_6$ (0.1 M) and $AgNO_3$ (0.005 M). All three electrodes were immersed in a CH_2Cl_2 solution (5 mL) containing $(n\text{-}Bu)_4NPF_6$ (0.1 M) as a support electrolyte and the analyte (7.7 mM for $[\mathbf{1}]^+OTf^-$, 7.3 mM for $[\mathbf{2}]^+OTf^-$). The electrolyte was dried under vacuum prior to use. In all cases, ferrocene was used as an internal standard, and all reduction potentials are reported with respect to the $E_{1/2}$ of the Fc/Fc^+ redox couple.

Crystallography. The crystallographic measurements were performed by using a Bruker APEX2 diffractometer, with graphite-monochromated Mo Kα radiation (λ = 0.71069 Å). Specimens of suitable size and quality were selected and mounted onto glass fiber with apiezon grease. The structures were solved by direct methods, which successfully located most of the non-hydrogen atoms. Subsequent refinement on F^2 with use of the SHELXTL/PC package (version 5.1) allowed location of the remaining non-hydrogen atoms. A summary of the pertinent crystallographic data follows:

Crystal data for $[\mathbf{1}]^+OTf^-$: $C_{26}H_{32}BF_3N_2O_3S$, M_r = 520.41, T = 140 K, space group $P\bar{1}$, triclinic, a = 8.2944(8) Å, b = 10.4347(10) Å , c = 16.1597(15) Å, α = 104.6880(10)°, β = 96.8560(10)°, γ = 100.4320(10)°, V = 1310.3(2) Å^3, Z = 2, D_c = 1.319 g cm^{-3}, μ(Mo Kα) = 0.175 mm^{-1}, 15106 reflections measured, 6033 unique (R_{int} = 0.0306), R_1 = 0.0575, wR_2 = 0.1185.

Crystal data for $[\mathbf{2}]^+OTf^- \cdot (OEt_2)_{0.5}$: $C_{30}H_{43}BF_3N_4O_{3.5}S$, M_r = 615.55, T = 140 K, space group $P\bar{1}$, triclinic, a = 8.110(3) Å, b = 13.043(4) Å, c = 15.489(5) Å, α = 85.454(3)°, β = 78.149(3)°, γ = 83.434(4)°, V = 1590.4(9) Å^3, Z = 2, D_c = 1.285 g cm^{-3}, μ(Mo Kα) = 0.158 mm^{-1}, 11305 reflections measured, 5861 unique (R_{int} = 0.0295), R_1 = 0.0841, wR_2 = 0.1276.

Acknowledgment. This work was supported by NSF (CHE-0646916), the Welch Foundation (A-1423), and the Petroleum Research Funds (Grant 44832-AC4).

Supporting Information Available: Computational details and crystallographic data in CIF format. This material is available free of charge via the Internet at http://pubs.acs.org.

OM701249N